Journal of
NANOSTRUCTURES
JNS
NANOSTRUCTURES
JNS.kashanu.ac.ir

Crystallization Kinetics and Characterization of Nanostructure Mica Glass-Ceramics with Optical Transparency

V. Khani, P. Alizadeh*

Department of Materials Science and Engineering, Tarbiat Modares University, Tehran, Iran

Article history:
Received 11/1/2014
Accepted 20/2/2014
Published online 1/3/2014

Keywords:
Glass Ceramics
Transparent
Mica
Nanostructure
Crystallization kinetics

**Corresponding author:*
E-mail address:
p-alizade@modares.ac.ir
Phone: 98 21 82884399
Fax: +98 21 82884390

Abstract

Transparent glasses in a system of Li_2O-MgO-SiO_2-Al_2O_3-F chemical constituents were prepared by melt quenching method. In the fabrication of nanocrystal glass-ceramics, controlled nucleation and subsequent crystal growth were necessary to avoid loss of transparency. It was therefore important to understand thermal properties and crystallization kinetics of the glass ceramics. The crystallization behavior of the prepared glass was investigated by DTA, XRD and SEM. By crystallization heat-treatment, various crystalline phases, microstructure and transmittance were obtained. The sellaite was first precipitated as the nuclei before the crystallization of mica and then mica nanocrystals were precipitated with average size of <40 nm. In this respect, the nucleation process was optimized in order to achieve a fine mica microstructure.

1. Introduction

Glass-ceramics are polycrystalline ceramic materials formed through the controlled crystallization of glasses by specific heat treatment. The bulk chemical composition, final phase association and microstructure are the most important factors affecting their final technical properties.

Transparent glass-ceramics (TGC) are obtained under several conditions, where the low optical absorption and scattering should be assured. When the crystals are small enough or the refractive index difference between the crystalline phases and the residual glass is very small, the glass-ceramics show transparency [1]. TGCs have received much attention because of practical applications in telescope mirrors [2], solid state lasers [3], solar cells and photonic devices [4, 5].

In fabrication of nanocrystal glass-ceramics, controlled nucleation process and crystal growth are important aspects to ensure maximum transparency. It is therefore important to understand thermal properties and crystallization kinetics of the glass-ceramics [6].

Mica glass-ceramics are the typical machinable materials. These glass-ceramics also exhibit

favorable thermal and electrical properties [7]. So these materials have found wide applications, e.g., vacuum feed throughs, windows for microwave-type parts, boundary retainers on the space shuttle and so on [7]. Glass-ceramics acquired as transparent materials are considered as novel machinable and optical materials [8]. In many applications the articles should be cut mechanically to achieve desired shapes and joined with other kinds of materials for device fabrications, thus, the mechanical and thermal properties of the articles are important [9,10]. Although transparent lithium-mica glass-ceramics have been studied [11-13], but their crystallization behavior is scarcely investigated. The objective of this work was to prepare transparent glass-ceramics with Li-mica nanocrystals and to study the crystallization behavior of these glass-ceramics. In order to obtain a fine microstructure with a large quantity of mica crystals a two-step heat-treatment was used. The effect of nucleation process on crystalline phases and microstructure was investigated and the optimum conditions of these processes were determined.

2. Materials and methods

The theoretical composition of based glass was 46.46 mol% SiO_2, 8.76 mol% Al_2O_3, 20.04 mol% MgO, 9.52 mol% Li_2O and 15.20 mol% MgF_2 [12]. The raw materials used in the preparation of glass were all high quality reagents of SiO_2, Al_2O_3, Li_2CO_3, $Mg(OH)_2$ and MgF_2. The thoroughly mixed glass batch was preheated at 900 ˚C for 1 h and then melted in a sealed platinum container at 1450 ˚C for 30 min in an electric furnace. The melt was cast into the pre-heated stainless steel mold. The obtained glass was annealed at about its glass transition temperature and cooled at rate of 2˚C/min to eliminate any residual strain. The obtained glasses were transparent and appeared as macroscopically homogeneous. The glasses prepared were crystallized by one-step and two-step heat-treatment methods.

In order to determine a suitable nucleation temperature and its subsequent thermal properties the dilatometric analysis was performed on the glass samples. The glass transition temperature (T_g), dilatometric softening point (T_d) and thermal expansion coefficient (α) were determined by dilatometric analysis (Netzsch DIL 402E).

The kinetics of crystallization of glasses was studied by a non-isothermal method. The thermal behavior of glasses was monitored by DTA scans which were carried out using a simultaneous thermal analyzer (Polymer Laboratories STA-1640). The glass powder with the weight of 15 mg was placed into a platinum crucible and α-Al_2O_3 was chosen as reference material. The samples were heated in air from ambient temperature to 1200 ˚C at heating rates of 10, 20, 30 and 40˚C/min.

The crystalline phases in the heat-treated samples were analyzed by XRD (X´pert MPD) using Cokα radiation, produced at 40 kV and 30 mA, with 2θ=2-80˚. For FESEM (Hitachi S-4160) observation, the samples were polished by diamond slurry and chemically etched in 5% HF solution for 80s.

3. Results and discussion

3.1. Crystallization study

A typical DTA crystallization exotherm for the glass is shown in Fig. 1. The DTA curve shows several exothermic peaks indicating crystallization process. The first exothermic peak is referred to the crystallization of mica crystals as in Fig. 2. The other exothermic peaks are attributed to the

formation of other phases as forsterite, chondrodite and ß-spodumene.

The effect of temperature on crystallization of glass-ceramics is shown in Fig. 2, where the samples are crystallized by one-step heat-treatment method and then heated at 650-900 ˚C for 1 h. As it is shown in Fig. 2a the as-quenched glass does not show any peaks and therefore it is considered as an amorphous material. In this process, mica (Li-type fluorophlogopite, $LiMg_3AlSi_3O_{10}F_2$) is first precipitated at 650 ˚C though the diffraction peaks in the XRD pattern are small. By increases in temperature, the quantity of mica crystals is increased, and the maximum quantity is obtained at about 750˚C.

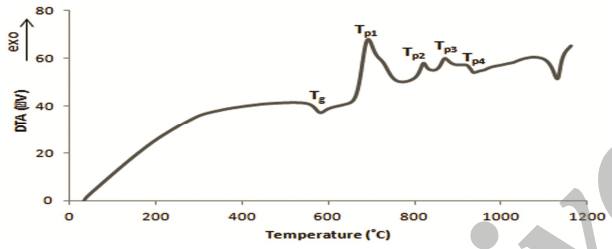

Fig. 1. DTA curve of the parent glass.

Mica is the main crystal at 650-750˚C although enstatite also is identified in XRD patterns. The amount of mica is reduced at higher temperatures and beyond 750˚C for longer times (≥4 h). $LiAlSi_3O_8$ is precipitated at 750 ˚C and then enstatite is disappeared at 800 ˚C and forsterite (Mg_2SiO_4) is crystallized. In the present work, there is a possibility of vaporization of fluorine during melting and crystallization of the glasses.

Kodaira et al. [15] reported also that fluorine deficiency causes fluormica compounds to decompose to forsterite and norbergite ($Mg_2SiO_4.MgF_2$). At temperatures up to 900 ˚C, chondrodite ($Mg_4(SiO_4)_2.MgF_2$) and ß-spodumene ($LiAlSi_2O_6$) are crystallized (Fig. 2).

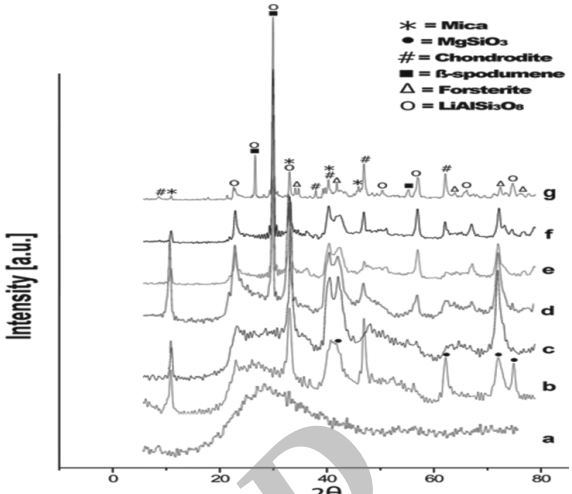

Fig. 2. XRD patterns of (a) glass and samples heated at: (b) 650 ˚C, 9(c) 700 ˚C, (d) 750 ˚C, (e) 800 ˚C, (f) 850 ˚C and (g) 900 ˚C for 1 h.

When a small amount of mica is precipitated in the samples, the contents of MgO and MgF_2 are decreased in the glasses and the glass compositions approach chemical compositions of other phases such as lithium aluminium silicate phases is easy to be precipitated as reported by Taruta et al. [11]. Although the quantity of mica crystals in glass ceramics increased with heating temperature, but their transparency was reduced (Fig. 3).

When the sample was heated at 650 ˚C it has a low quantity of mica crystals. So, in order to obtain a fine microstructure with a large quantity of mica crystals a two-step heat-treatment was used. In order to obtain a fine microstructure, the nucleation process was considered very important in controlling the crystallization process. The dilatometric analysis was performed on the glass sample for determination of suitable nucleation temperature. The values of T_g, T_d and α were obtained as 557 ˚C, 603 ˚C and 7.7×10^{-6} K^{-1}, in the given order. As the nucleation process is usually carried out at a temperature range between T_g and T_d therefore, temperature of 580°C was selected. The XRD analysis of the heat-treated sample at 580 ˚C showed that sellaite (MgF_2) was first

precipitated at 580 ˚C, as shown in Fig. 4. Next, mica was precipitated at higher temperatures. It is known that fluorophlogopite is precipitated through sellaite, chondrodite, norbergite, and/or mullite ($3Al_2O_3.2SiO_2$) [16]. Presumably, in the present work, sellaite must have precipitated instantaneously as the nuclei formation before the crystallization of mica. For determination of the optimum nucleation time, the samples were first nucleated at 580 ˚C for different durations and then crystallized at 650 ˚C for 4 h. The XRD patterns of these samples are shown in Fig. 5. One of the criteria considered for selection of the optimum time was the height of the mica peaks in XRD patterns. It is observed that increasing the time of nucleation results in increasing the crystallized mica at first and decreasing thereafter. At higher times of nucleation (>5 h), a decrease in amount of mica can be attributed to the probable coalescence of existing nuclei, giving rise to smaller nuclei population. So, the optimum condition for nucleation process was obtained at 580 ˚C for 5 h.

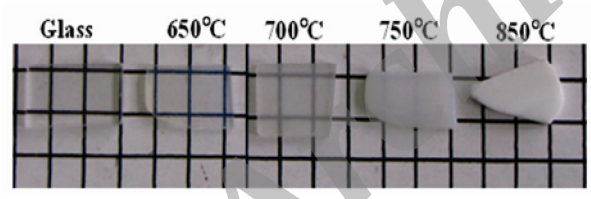

Fig. 3. Photographs of parent glass and glass-ceramics (heated at different times for 1 h).

3.2. Microscopic studies

Fig. 6a shows the micrographs of glass sample, taken by SEM. In the parent glass, a separation of droplet-like phase with 40-50 nm size range was observed, which was attributed to a binodal phase separation.

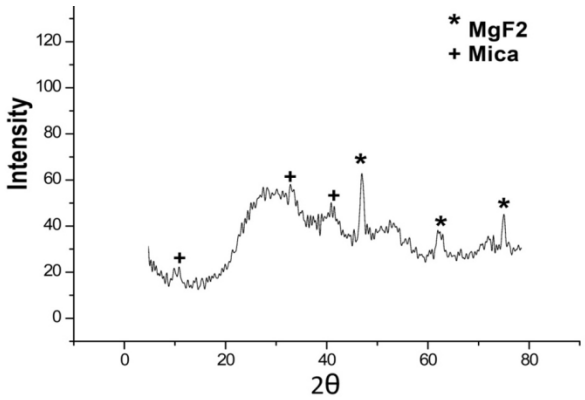

Fig. 4. XRD pattern of samples nucleated at 580 ˚C for 5 h.

Fine crystals, as shown in Fig. 6b, precipitated at 580 ˚C for 5 h. The crystals are of sellaite type as expected from the results by x-ray powder diffraction analysis.

Fig. 6c shows the SEM images of heat-treated samples obtained under optimum conditions. In this sample, aggregated particles with range of sizes 100-300 nm were precipitated uniformly. They were composed of fine particles with size of <40 nm. Measuring the crystallite size of the mica according to the Scherrer equation, the size was about 31 nm. Therefore, the fine particles corresponded to the mica crystallites and the glass-ceramic displayed a very good transparency.

Increase in temperature on the type of crystalline phases also affected their microstructure. The micrographs of these samples are shown in Fig. 7. At temperatures higher than 700 ˚C, the transparency of the samples was significantly reduced which was related to large increases in size of the crystals and volume fraction crystallized. The crystals at 900 ˚C grew to such an extent that plate-like mica crystals were quite visible.

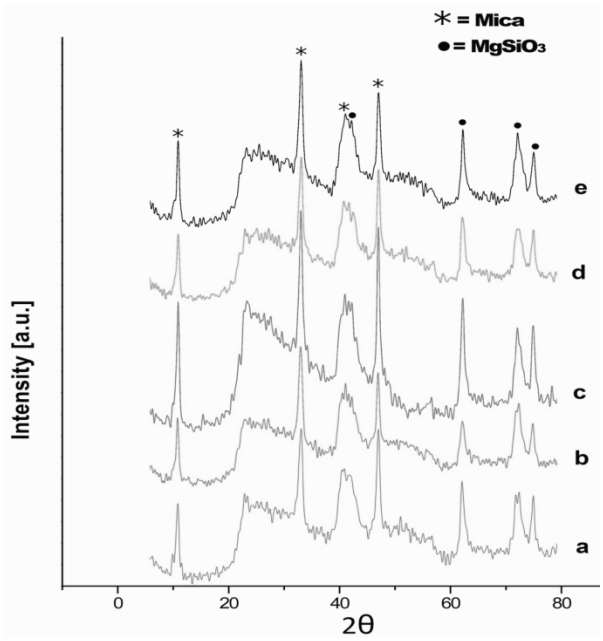

Fig. 5. XRD patterns of samples nucleated at 580 ˚C for (a) 1 h, (b) 3 h,(c) 5 h, (d) 7 h and (e) 9 h and heated at 650 ˚C for 4 h.

3.3. Transparency study

The photographs of the polished samples are shown in Fig. 3. As the heating temperature is increased, the samples lost the transparency. The visible ray transmittance of the samples is shown in Fig. 8. It is clear that the transparency of glass-ceramics is reduced by the heat treatment. That is, nanocrystals precipitated in the glass-ceramic samples can scatter the visible ray, particularly, a light of lower wavelengths. The transmittance of TGC depends on the degree of crystallinity and crystal size. The samples heat-treated at higher temperatures have relatively larger crystallites with higher volume fraction crystallized, resulting in semi-transparency and opacity. The transmittance of the glass-ceramic was improved by a two-step heat-treatment method. Because many nuclei were precipitated in the sample by heating at 580 ˚C, it resulted in finer microstructure. Therefore, the heated sample showed higher transmittance.

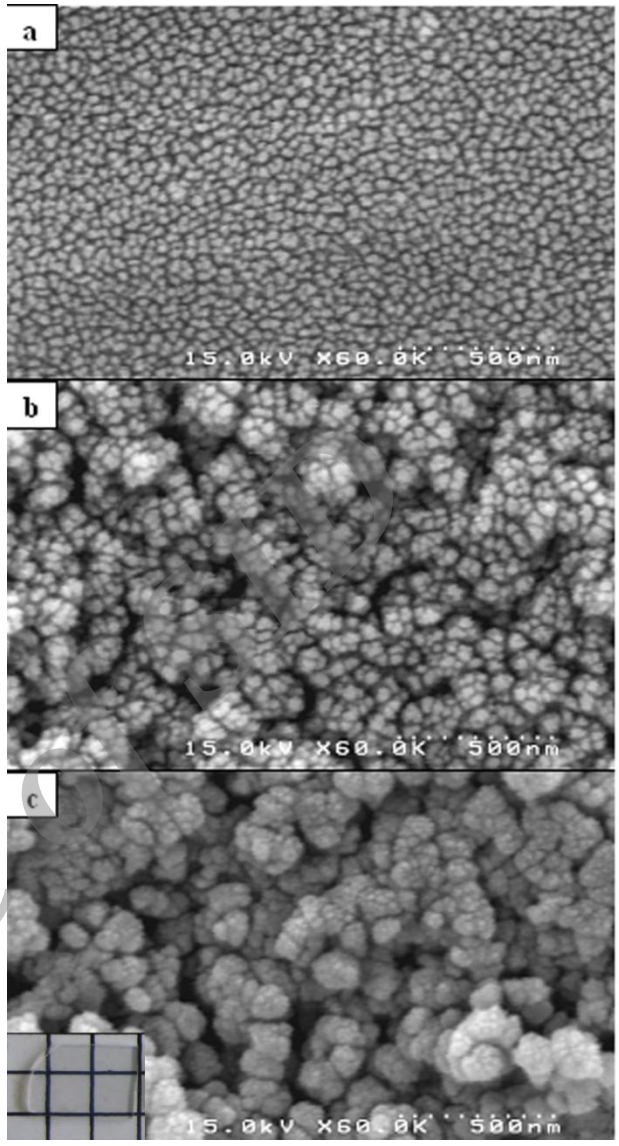

Fig. 6. SEM photographs of the samples a) glass, b) nucleated at 580 ˚C for 5 h and c) nucleated at 580 ˚C, 5 h and crystallized at 650 ˚C, 4 h, the glass-ceramics produced under optimum conditions has very good transparency.

3.3. Activation energy (E_c) and Avrami parameter (n) of parent glass

For determination of the crystallization mechanism DTA measurements were performed using two different particle sizes (180-210μm and <45μm). In glasses with surface nucleation, the

crystallization peak position is strongly dependent upon the particle size.

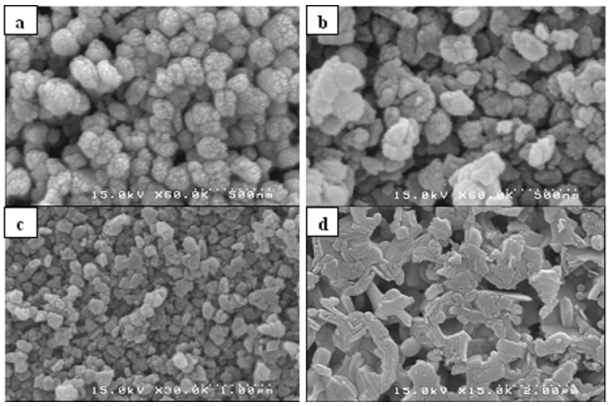

Fig. 7. SEM photographs of the samples heated at (a) 700 ˚C, (b) 750 ˚C, (c) 800 ˚C and (d) 900˚C for 1 h.

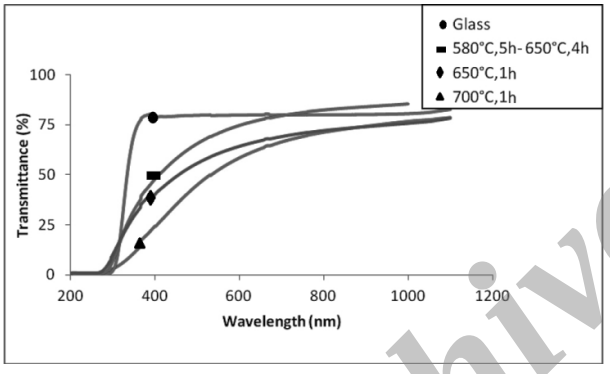

Fig. 8. The optical transmission spectra for glass, the samples prepared by two-step heat-treatment method (nucleated at 580 ˚C, 5 h and heated at 650 ˚C, 4 h), and the samples prepared by one-step heat-treatment method, 650 ˚C,1 h and 700 ˚C, 1 h. The transparency of glass-ceramic is improved by two-step heat-treatment method.

The fine samples with high surface areas are crystallized at lower temperatures, but in bulk nucleation mechanism the position of the exothermic peak is almost independent from particle size [17]. The similar DTA curves, observed in samples with different particle sizes (low ΔT_p), indicate that there are no major changes between the DTA results of different samples; revealing no dependency of the surface and, therefore, pointing to the occurrence of bulk crystallization.

Fig. 9 Shows the DTA curves of the glass at the heating rate of 10, 20, 30 and 40 ˚C/min. The glass transition temperature (T_g), onset crystallization temperature (T_{on}) and crystallization peak temperature (T_p) for the first peak determined from the DTA curves are listed in Table 1. The values of T_g, T_{on} and T_p are shifted to higher temperatures with increasing heating rate.

In order to confirm the mechanism of crystallization the modified Kissinger and the modified JMA equations [18-20] (Eqs. (1) and (2), respectively) were used.

$$Ln(\alpha^n/T_p^2) = -mE_c/RT_p + \text{constant} \quad (1)$$

Where α and T_p are heating rate and crystallization peak temperature, respectively. Other parameters which are usually considered for determination of the crystallization mechanism [21-23] are the Avrami parameter (n) and the crystal growth dimensionality (m), where m is defined as n-1.

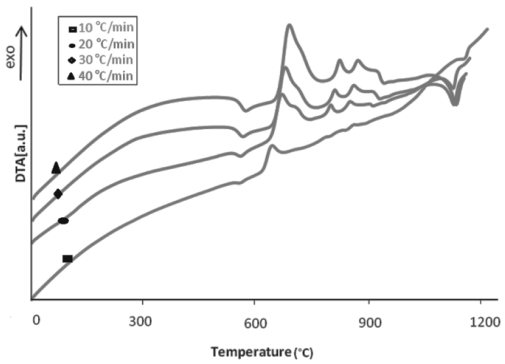

Fig. 9. DTA curves for glass sample recorded at different heating rates ranging from 10 to 40 ˚C /min.

$$Ln[-Ln(1-x)] = -nLn\alpha - mE_c/RT + \text{constant} \quad (2)$$

Where *x* is the fraction crystallization at each temperature and can be calculated by the ratio of partial area to total area of the crystallization peak.

The value of *n* can be calculated from Eq. (2), plot of Ln[-Ln(1-x)] versus Lnα is expected to be linear, and from the slope of plot the Avrami parameter is calculated (Fig. 10).

Table 1. The values of T_g, T_{on} and T_p of the glass for different heating rates

A (˚C/min)	T_g (˚C)	T_{on} (˚C)	T_p (˚C)
10	557	625	655
20	566	645	683
30	569	650	691
40	573	665	700

Plot of $Ln(\alpha^n/T_p^2)$ versus $(1/T_p)$ also is expected to be linear, and from the slope of the plot, the activation energy, E_c can be obtained (Fig. 11). In this study n and E_c values were determined as 2.93 and 338.57 kJ/mol, respectively. The Avrami constant (n) indicates two-dimensional bulk crystallization.

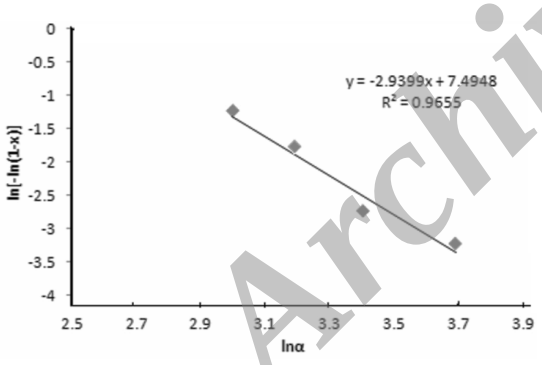

Fig. 10. Variation of Ln [-Ln(1-x)] vs. heating rate logarithm (lnα).

3.4. Transition activation energy (E_t) of parent glass

The relationship between T_g and α can be discussed through the e mpirical equation:

$$T_g = C_1 + C_2 \ln\alpha \quad (3)$$

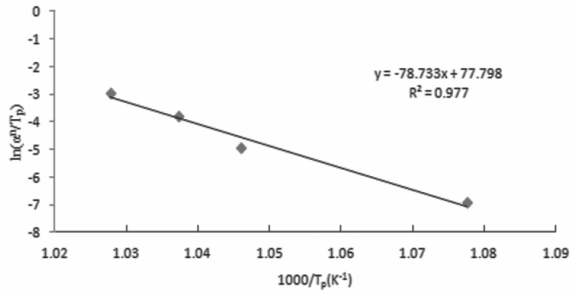

Fig. 11. Determination of crystallization activation energy.

Where, C_1 and C_2 are constants for a given glass composition [24, 25]. To obtain the activity energy of glass transition, E_t, the Kissinger method is commonly used [24]. According to the Kissinger equation, the glass transition temperature depends on the heating rate as follows:

$$Ln(\alpha/T_g^2) = -E_t/RT_g + \text{constant} \quad (4)$$

Plot of T_g versus lnα for the glass, the values of C_1 and C_2 can be obtained by using the least square fit, and this equation holds good for the studied samples (Fig. 12). Based on the Eq. (4), slope of plot of $Ln(\alpha/T_g^2)$ versus $(1/T_g)$ for the parent glass yield the value of E_t/R where E_t corresponds to the glass transition activation energy (as shown in Fig. 13). From Figs. 12 and 13, for the glass, T_g =11.25 lnα +804.38 and E_t =498.9 kJ/mol.

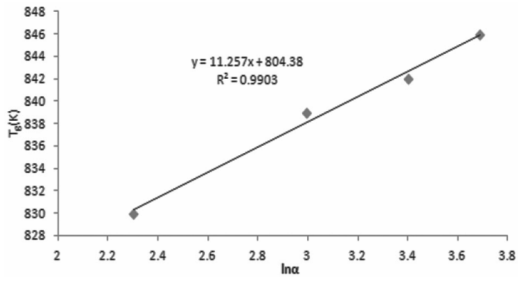

Fig. 12. Plot of T_g vs. lnα for the parent glass.

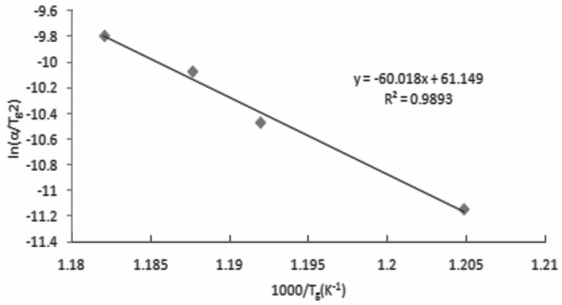

Fig. 13. Plot of $Ln(\alpha/T_g^2)$ vs. $1/T_g$ for the parent glass.

4. Conclusion

The objective of this work was fabrication of mica glass-ceramics with good transmittance in the visible region and to study the crystallization behavior of these glass-ceramics. In order to obtain a fine microstructure with a large quantity of mica crystals a two-step heat-treatment was used. The effect of nucleation process on crystalline phases and microstructure was investigated and the optimum conditions of these processes were determined.

Li-mica nanocrystals with average size of <40 nm were formed using a two-step heat-treatment. The optimum conditions for nucleation process of mica phase were determined. The transparency of the samples was improved by a two-step heat-treatment method, and at high temperatures with enlargement and changes in crystal morphology, the samples were opaque. The kinetic parameters, such as crystallization activation energy, Avrami exponent and glass transition activation energy were determined as 338.57, 2.93 and 498.9 kJ/mol, respectively. The *n* value indicated to a two-dimensional bulk crystallization mechanism.

References

[1] G.H. Beall, L.R. Pinckney, J. Am. Ceram. Soc. 82 (1999) 5-16.

[2] G. Partridge, in: New Materials and Their Applications, ed. S.G. Burnay, Institute of Physic Conference Series No. 89: Session 4 (Institute of Physics, Pittsburgh, PA, 1987) P. 161.

[3] G. Muller and N. Neutoth, J. Appl. Phys. 44 (1973) 2315.

[4] N.F. Borrelli, J. Appl. Phys. 38 (1967) 4243.

[5] N.F. Borrelli and M.M. Layton, J. Non-Cryst. Solids 6 (1971) 197.

[6] H. Tanak, M. Yamamoto, Y. Takahashi, Y. Benino, T. Fujiwara, T. Komatsu, Optical Materials 22 (2003) 71-79.

[7] W. Holland, G. Beall, Glass-Ceramics Technology, The American Ceramic Society, 2002.

[8] S. Taruta, Y. Iwasaki, H. Nishikiori, T. Yamakami, T. Yamaguchi, K. Kitajima, K. Okada J. Mater. Sci. Eng. B, 177 (2012) 504-509.

[9] V. Khani, P. Alizadeh, M.S. Shakeri, Mater. Res. Bulletin 48 (2013) 3579–3584.

[10] V. Khani, P. Alizadeh, Phys. Chem. Glasses: Eur. J. Glass Sci. Technol. B, 54 (2) (2013) 104–108.

[11] S. Taruta, T. Ichinose, T. Yamaguchi, K. Kitajima, J. Non-Cryst. Solids 352 (2006) 5556-5563.

[12] S. Taruta, M. Suzuki, T. Yamaguchi, K. Kitajima, J. Non-Cryst. Solids 354 (2008) 848–855.

[13] S. Taruta, M. Matsuki, H. Nishikiori, T. Yamakami, T. Yamaguchi, K. Kitajima, J. Ceram. Int. 36 (2010) 1303-1309.

[14] Lj. Radonjic, Lj. Nikolic, J. Eur. Ceram. Soc. 7 (1991) 11-16.

[15] K. Kodaira, H. Fukuda, S. Shimada, T. Matushita, J. Mater. Res. Bull. 19 (1984) 1427-1432.

[16] C.K. Chyung, G.H. Beall, D.G. Grossman, Electron microscopy and structure of materials, in: Proceedings of 5th International Materials Symposium. University of California, Barkeley, CA, 1971, p. 1167.

[17] P. Alizadeh, V.K. Marghussian, J. Eur. Ceram. Soc.20 (2000) 765-773.
[18] H.E. Kissinger, Anal. Chem. 11 (1957) 1702-1706.
[19] K. Matusita, S. Sakka, J. Non-Cryst. Solids, 38-39 (1980) 741-746.
[20] J. Malek, J. Thermochimica Acta, 267, (1995) 61-73.
[21] M. Rezvani, B.E. Yekta, V.K. Marghussian, J. Eur. Ceram. Soc. 25 (2005) 1525-1530.
[22] Y. Cheng, H. Xiao, W. Guo, W. Guo, J. Thermochimica Acta, 444, (2006) 173-178.
[23] A. Marotta, A. Buri, J. Thermochimica Acta, 25, (1978) 155-160.
[24] C. Liu, G. Tang, L. Luo, W. Chen, J. Alloys Compd. 474 (2009) 468-472.
[25] M. Lasocka, Mater. Sci. Eng. 23 (1976) 173-177.

Crystallization Kinetics and Characterization of Nanostructure Mica Glass Ceramics with Optical Transparency

V. Khani, P. Alizadeh*

Department of Materials Science and Engineering, Tarbiat Modares University, Tehran, Iran

سینیتیک کریستالیزاسیون و و شناسایی نانوساختار شیشه میکا- سرامیک با شفافیت نوری

چکیده

شیشه شفاف در یک سیستمی از Li_2O-MgO-SiO_2-Al_2O_3-F ترکیبات شیمیایی بوسیله روش ذوب کوئنچینگ آماده شد. در ساخت نانو کریستال شیشه-سرامیک ، کنترل هسته زایی و متعاقب آن رشد بلور برای اجتناب از کاهش شفافیت ضروری بود. بنابراین دانستن خواص حرارتی و سینتیک تبلور سرامیک شیشه ای مهم بود. رفتار تبلور شیشه آماده شده بوسیله XRD،DTA و SEM بررسی شد. بوسیله تبلور حرارتی ، فازهای متفاوت بلورین، میکروساختار ها و درصد عبور قابل دستیابی شد. ابتدا سلایت به عنوان هسته قبل از تبلور میکا رسوب داده شد وسپس نانو کریستال های میکا با سایز میانگین کمتر از ۴۰ nm رسوب داده شدند. در این رابطه فرایند هسته زایی به منظور دستیابی به میکروساختار خوب میکا بهینه سازی شد.